Electronic Supplementary Information

Self-assembly of benzophenone-diphenylalanine conjugate into nanostructured photocatalyst

Simone Adorinni,[a] Giulio Goti,[b] Lorenzo Rizzo,[b] Federica Grassi,[b] Slavko Kralj,[c,d] Fatima Matroodi,[e] Mirco Natali,[f] Rita De Zorzi,[a] Silvia Marchesan,[*a] and Luca Dell'Amico[*b]

[a.] *Chemical and Pharmaceutical Sciences Dept., University of Trieste, V. Giorgieri 1, 34127 Trieste, Italy.*
[b.] *Chemical Sciences Dept., University of Padova, V. Marzolo 1, 35131 Padova, Italy.*
[c.] *Materials Synthesis Dept., Jožef Stefan Institute, Jamova 39, 1000 Ljubljana, Slovenia*
[d.] *Pharmaceutical Technology Dept., University of Ljubljana, Aškerčeva 7, 1000 Ljubljana, Slovenia*
[e.] *Elettra Sincrotrone Trieste, 34149 Basovizza, Trieste, Italy*
[f.] *Department of Chemical, Pharmaceutical, and Agricultural Sciences, University of Ferrara, V. Borsari 46, 44121 Ferrara, Italy.*

Table of contents

1. Material and Methods

2-Chlorotrytil resin, Fmoc protected L-phenylalanine were purchased from Iris Biotech GmbH, 3-benzoylbenzoic acid was purchased by Alfa Aesar and *O*-(benzotriazol-1-yl)-*N*,*N*,*N*′,*N*′-tetramethyluronium hexafluorophosphate (HBTU) and 1-hydroxy-7-azabenzotriazole (HOAt) were purchased from GL Biochem (Shanghai) Ltd. All solvents were purchased of analytical grade from Merck. Piperidine, trifluoroacetic acid (TFA), *N*,*N*-diisopropyl ethyl amine (DIPEA), triisopropyl silane (TIPS) were purchased from Merck. Other reagents and solvents were purchased at the highest commercial grade quality from Sigma Aldrich, FluoroChem, TCI or Janssen and used as received, unless otherwise stated. High purity Milli-Q-water (MQ water) with a resistivity greater than 18 M Ω cm was obtained from an in-line Millipore RiOs/Origin system. NMR spectra were recorded on Varian Innova Instrument, Bruker 400 AVANCE III HD equipped with a BBI-z grad probe head 5mm, Bruker 500 AVANCE III equipped with a BBI-ATM-z grad probe head 5mm, Bruker DPX 200 equipped with a QNP probehead, Bruker Avance 300 equipped with a BBO-z grad probehead or Bruker AVANCE Neo 600 equipped with a TCI Prodigy probehead. The chemical shifts (δ) for ^{1}H and ^{13}C are given in ppm relative to residual signals of the solvents ($CHCl_3$ @ 7.26 ppm for ^{1}H NMR and @ 77.16 ppm for ^{13}C NMR; DMSO @ 2.50 ppm for ^{1}H NMR and @ 39.52 ppm for ^{13}C NMR). Coupling constants are given in Hz. The following abbreviations are used to indicate the multiplicity: s, singlet; d, doublet; t, triplet; q, quartet; m, multiplet. NMR yields were calculated by using 1,3,5-trimethoxybenzene as internal standard. ESI-MS spectra were recorded on an Esquire 4000 – Bruker.

Chromatographic purifications of products were accomplished by flash chromatography on silica gel (SiO_2, 0.04-0.063 mm) purchased from Sigma-Aldrich, with the indicated solvent system according to the standard techniques. Thin-layer chromatography (TLC) analysis was performed on pre-coated Merck TLC plates (silica gel 60 GF254, 0.25 mm). Visualisation of the developed chromatography was performed by checking UV absorbance (254nm) as well as with aqueous potassium permanganate solutions. Organic solutions were concentrated under reduced pressure on a Büchi rotary evaporator.

The absorption of peptide and the interaction studies with the *E*-stilbene were measured using 0.1 mm quartz cell on an *Agilent-Cary 5000 UV-Vis-NIR* over a range of wavelengths from 800 to 200 nm. The other Steady-state absorption spectroscopy studies were performed at room temperature on a Varian Cary 50 UV-Vis double beam spectrophotometer; 10 mm path length Hellma Analytics 100 QS quartz cuvettes were used. Steady-state fluorescence spectra were recorded on a Varian Cary Eclipse Fluorescence spectrophotometer; 10 mm path length Hellma Analytics 117.100F QS quartz cuvettes were used. 77 K luminescence measurements were performed by freezing alcoholic solutions (ethanol/methanol, 4/1) and taken on an Edinburg Instrument spectrofluorometer. Time-resolved absorption measurements were performed with a custom laser spectrometer composed of a Continuum Surelite II Nd:YAG laser (FWHM = 6–8 ns) with a frequency tripled (355 nm, 160 mJ) option. Light transmitted by the sample was focused onto the entrance slit of a 300 mm focal length Acton

SpectraPro 2300i triple grating, flat field, double exit monochromator equipped with a photomultiplier detector (Hamamatsu R3896). Signals from the photomultiplier were processed by means of a Teledyne LeCroy 604Zi (400 MHz, 20 GS/s) digital oscilloscope.

Time-Correlated Single Photon Counting (TC-SPC). Fluorescence lifetimes were measured using a TC-SPC apparatus (PicoQuant Picoharp 300) equipped with subnanosecond LED sources (280, 380, 460, and 600 nm, 500-700 ps pulse width) powered by a PicoQuant PDL 800-B variable (2.5-40 MHz) pulsed power supply. The decays (blue traces) were analysed by means of PicoQuant FluoFit Global Fluorescence Decay Analysis Software using a deconvolution procedure accounting for the instrumental response factor (IRF, red traces).

390 nm Kessil PR160L light was used to perform photochemical reactions. The emission spectra reported here can be found at www.kessil.com/science/PR160L.php

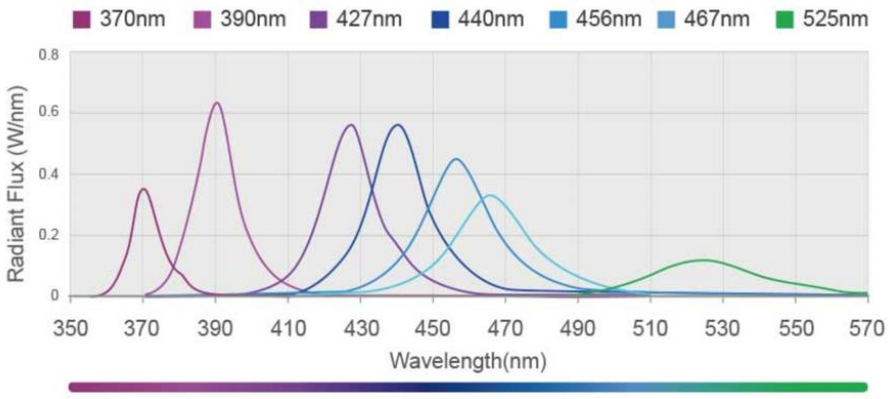

Figure S1: Emission spectra of Kessil lights. The 390 nm lamp was used in this work.

2. Synthesis and characterisation of BP-Phe-Phe photocatalyst (1)

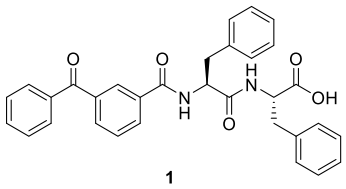

1

Benzophenone-L-Phe-L-Phe-COOH **1** was synthesised following Fmoc-based solid-phase peptide synthesis (SPPS). The resin (2-chlorotrytil chloride, 500 mg) was swelled in dichloromethane (5 mL) for 30 minutes, Then $SOCl_2$ (50 µL) was added, and the reaction was shaken under an argon flow for 1 h at room temperature. After that, the resin was washed with DMF (2x5 mL) and dichloromethane (2x5 mL). Next, a solution of Fmoc-L-Phe-OH (309.9 mg, 0.8 mmol), DIPEA (450 µL) in DMF/dichloromethane (3:2) was added to the resin, and the reaction was stirred for 1.5 h. Then, methanol (1 mL) was added and it was shaken for 5 minutes following by washes with DMF (3x5 mL) and dichloromethane (3x5 mL). For the deprotection, piperidine 20% in DMF (5 mL) was added to the reactor and was stirred at room temperature (2x7 minutes). The reaction mixture was washed with DMF and dichloromethane. For the first coupling, a mixture of Fmoc-L-Phe-OH (929.8 mg, 2.4 mmol), HBTU (758.2 mg, 2.0 mmol), HOAt (272.2 mg, 2.0 mmol) and DIPEA 1 M in DMF (1 mL) was ultrasonicated until the solution was clear, and was added to the reactor. The coupling was shaken at room temperature for 1.5 h. Then, the resin was washed and deprotected as in the previous step. The coupling and deprotection of the following amino acid (L-Phe) was done exactly in the same way as the first coupling, by using Fmoc-L-Phe-OH (929.8 mg, 2.4 mmol). For the introduction of benzophenone motif, a coupling was performed under the same conditions 3-benzoylbenzoic acid and performing the coupling for 3 hours. Eventually, the peptide was cleaved from the resin by shaking 2 hours in the presence of a solution of TFA/dichloromethane/H_2O/triisopropylsilane (47.5/47.5/2.5/2.5) (10 mL). The solution was drained from the reactor, and the solvent was evaporated under air flow. The peptide was purified dissolving the reaction's crude into a mixture of acetonitrile/H_2O (70:30) and the mixture was spinned. Finally, the solid was triturated in diethyl ether, filtered and washed three times with diethyl ether. The solid was collected in falcons and then freeze-dried obtaining benzophenone-L-Phe-L-Phe-COOH **1** as a white fluffy powder (354.0 mg, 85% yield, mp 208.0±0.4 °C yellow solution).

^{1}H NMR (400 MHz, DMSO-d_6) δ 12.77 (s, 1H$_g$), 8.78 (d, J = 8.6 Hz, 1H$_a$), 8.35 (d, J = 7.8 Hz, 1H$_d$), 8.10 (t, J = 1.6 Hz, 1H, Ar$_{BP}$), 8.07 – 8.01 (m, 1H, Ar$_{BP}$), 7.90 – 7.83 (m, 1H, Ar$_{BP}$), 7.78 – 7.56 (m, 6H, Ar$_{BP}$), 7.34 – 7.28 (m, 2H, Ar$_{FF}$), 7.27 – 7.10 (m, 8H, Ar$_{FF}$), 4.75 (ddd, J = 11.2, 8.6, 3.8 Hz, 1H$_b$), 4.48 (td, J = 8.5, 5.2 Hz, 1H$_e$), 3.09 (dt, J = 13.6, 4.5 Hz, 2H$_c$), 3.01 – 2.87 (m, 2H$_f$).

^{13}C NMR (101 MHz, DMSO-d_6) δ 195.1, 172.4, 171.1, 165.2 (4xCO), 138.0, 137.2, 136.8, 136.5, 134.1, 132.8, 131.9, 131.1, 129.5, 128.9, 128.5, 128.2, 127.9, 127.8, 126.2, 126.0, 54.4, 53.3, 36.6, 36.4.

ESI-MS: *m/z* calculated for M = 520.2, observed positive mode [M + Na]$^+$ = 543.2 and negative mode [M – H]$^-$ = 519.2

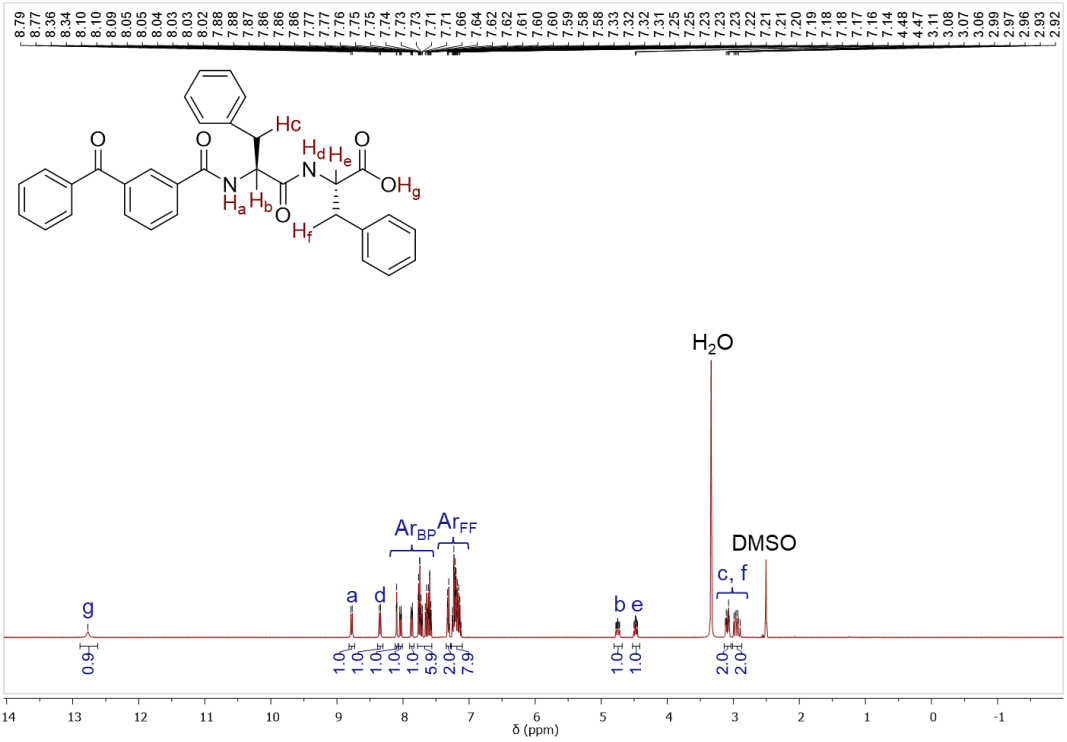

Figure S2:^{1}H NMR spectrum of BP-Phe-Phe.

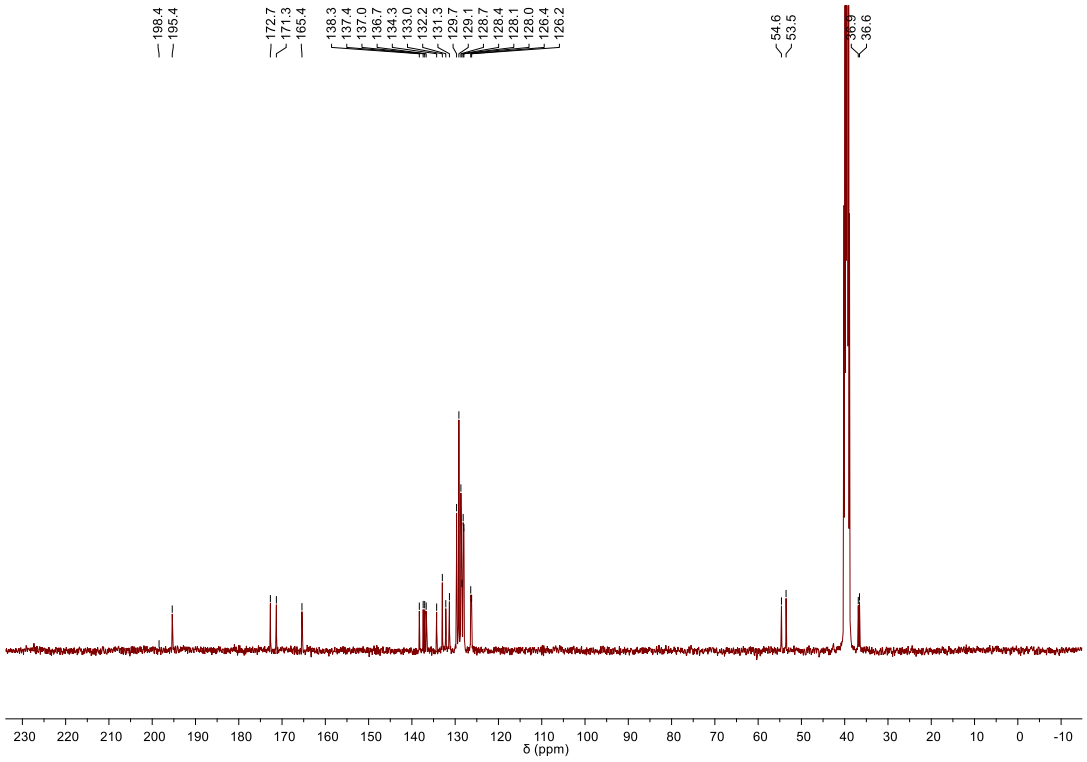

Figure S3: ^{1}H NMR spectrum of BP-Phe-Phe.

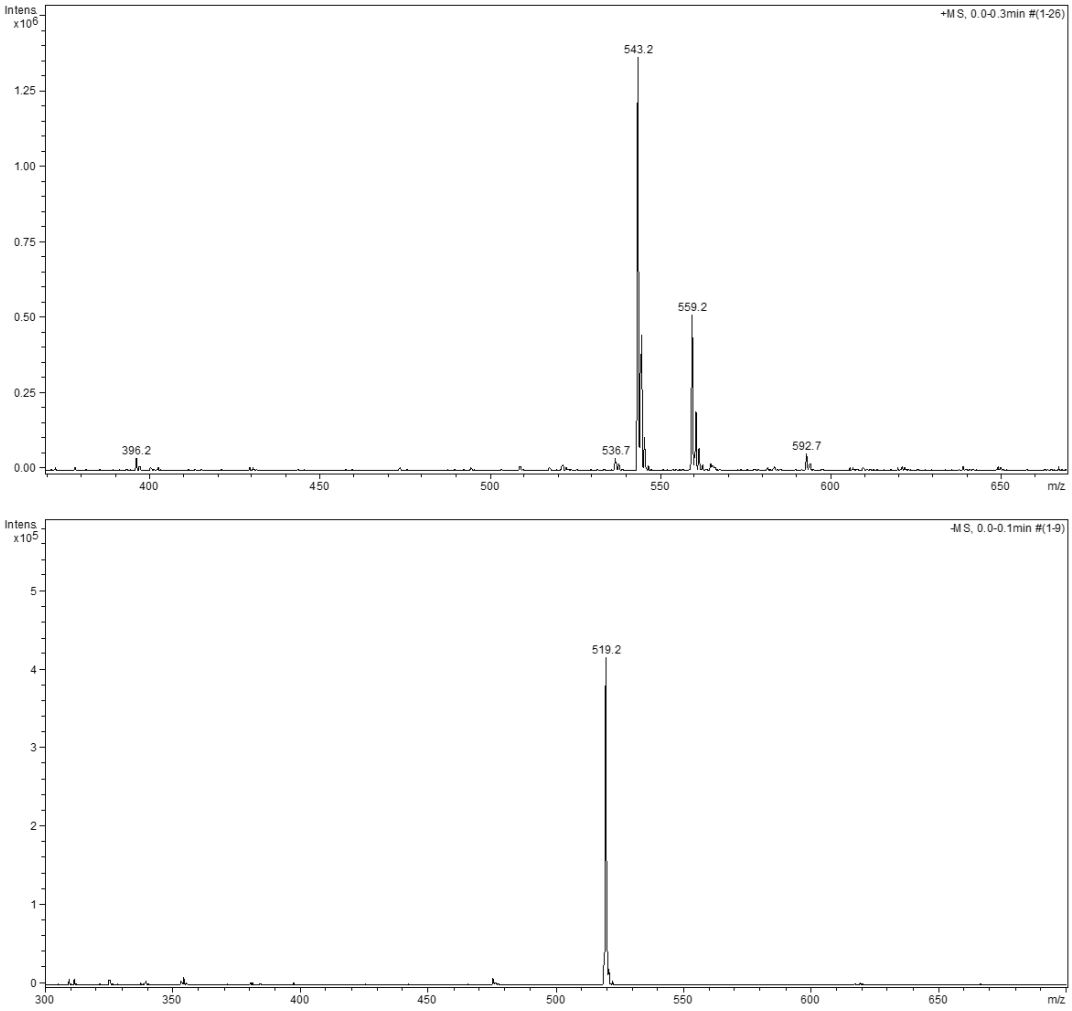

Figure S4: ESI-MS spectra of BP-Phe-Phe (positive ion mode, top, negative ion mode, bottom).

3. Synthesis and characterisation of BP methyl ester photocatalyst (4)

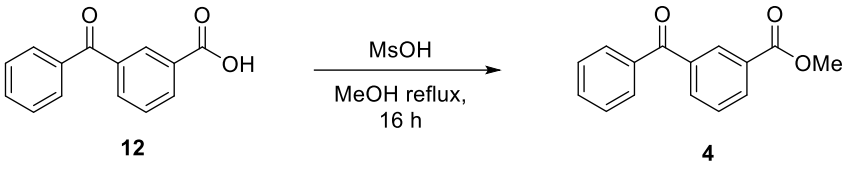

12 **4**

Methanesulfonic acid (48 mg, 0.5 mmol) was added to a solution of 3-benzoylbenzoic acid **12** (570 mg, 2.5 mmol) in anhydrous methanol (4 mL) under inert atmosphere (N_2), and the mixture was heated under a gentle reflux overnight (16 h) to have a complete conversion of the reagent.[1] The disappearance of the starting compound was checked by TLC: petroleum ether:Et_2O, 4:1. Then, H_2O was added and the mixture extracted with EtOAc (4x). The reunited organic phase was concentrated in vacuo. The crude material was purified by flash chromatography (Hex:Et_2O = 8:2) to get **4** as a colourless oil. After some hours in freezer, a transparent solid is obtained. Analytical data are in agreement with the literature.[1,2]

^{1}H NMR (500 MHz, $CDCl_3$) δ 8.44 (s, 1H), 8.26 (d, *J* = 7.8 Hz, 1H), 8.01 (d, *J* = 7.7 Hz, 1H), 7.80 (d, *J* = 7.0 Hz, 2H), 7.65 – 7.55 (m, 2H), 7.51 (t, *J* = 7.7 Hz, 2H), 3.94 (s, 3H).

^{13}C NMR (50.3 MHz, $CDCl_3$) δ 138.0, 130.9, 130.4, 132.8, 128.6, 134.0, 166.2, 52.3, 195.6, 137.1, 130.0, 128.5, 133.2 [(45)].

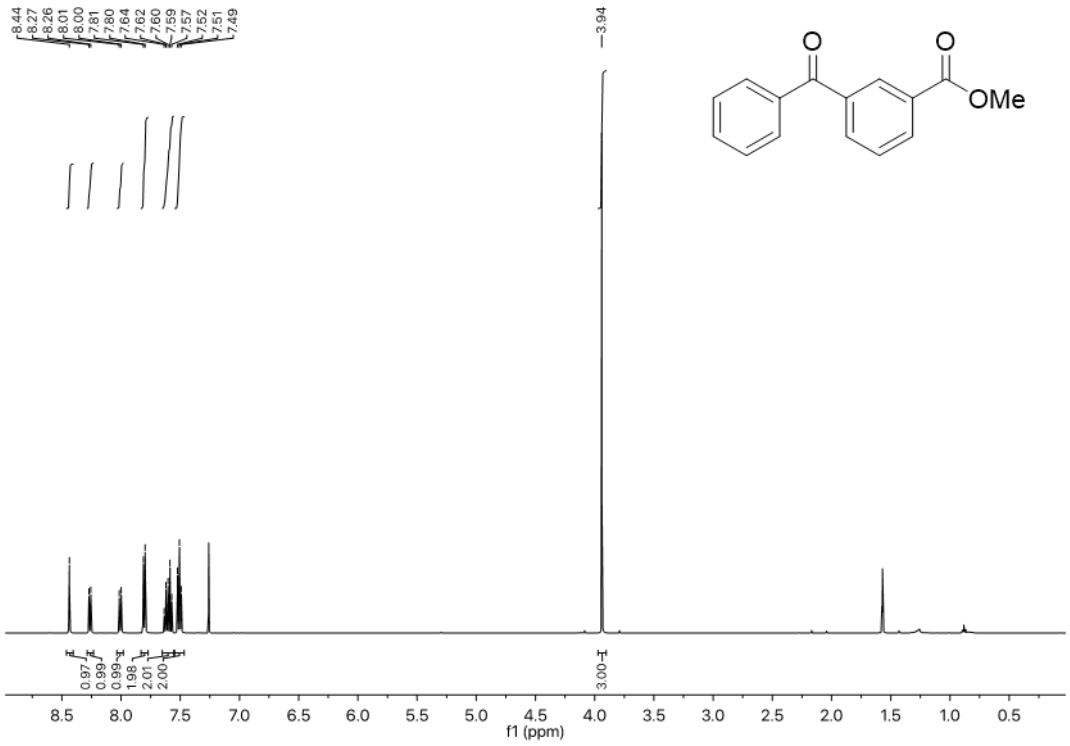

*Figure S5: ^{1}H NMR spectrum of BP methyl ester **4**.*

4. Self-assembly test

The self-assembled peptide was obtained by dissolving the peptide in 10 % of 1,1,1,3,3,3-hexafluoro-2-propanol (HFIP). After complete dissolution, 90 % of CH_3CN was added to the solution containing the peptide. All the experiments were performed at room temperature. The solvents tested are reported in **Table S1**.

Solvents	Concentration (mM)	Comments
CH_3CN: HFIP 90:10	1.0 mM	Nothing at visual observation
	2.5 mM	Fibers
	5.0 mM	Fibers
	7.5 mM	Fibers
	10 mM	Fibers
	20 mM	Fibers
H_2O: HFIP 90:10	1.0 mM	A solid precipitate immediately formed after the addition of water
	5.0 mM	A solid precipitate immediately formed after the addition of water
	10 mM	A solid precipitate immediately formed after the addition of water
	15 mM	A solid precipitate immediately formed after the addition of water
Acetone	2.5 mM	Nothing at visual observation

Table S1. Self-assembly test of BP-Phe-Phe.

5. Transmission Electron Microscopy (TEM)

For the preparation of the samples for transmission electron microscopy (TEM), copper-lacey carbon film grids were used after the exposure to UV-Ozone cleaner (*UV-Ozone Procleaner Plus*) for 5 minutes in order to increase surface hydrophilicity. TEM images were acquired using Jeol JEM 2100 (Japan) instrument at 100 kV. Average diameter of the nanostructures was derived considering at least 100 objects from various micrographs.

- Fibers at 5 mM

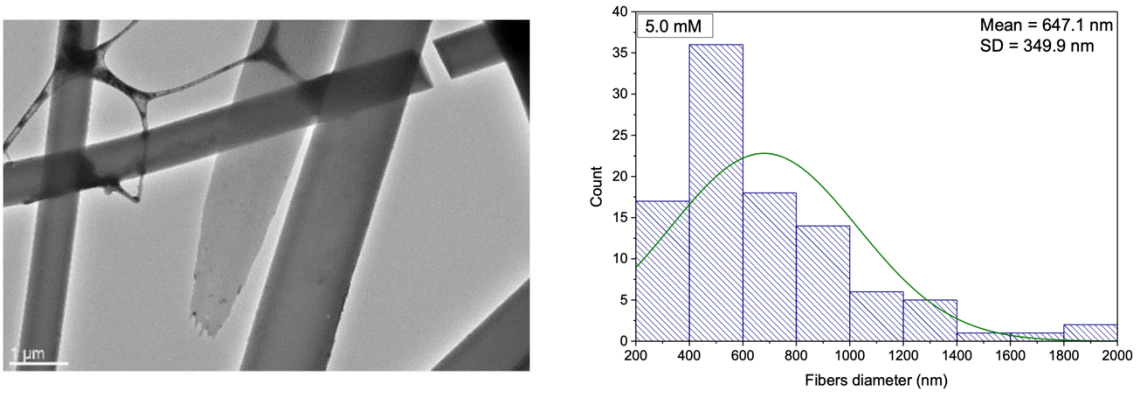

Figure S6: TEM micrographs for BP-Phe-Phe fibrils at 5 mM (left). Gaussian distribution of BP-Phe-Phe fibril diameter at the concentration of 5 mM (right).

- Fibers at 7.5 mM

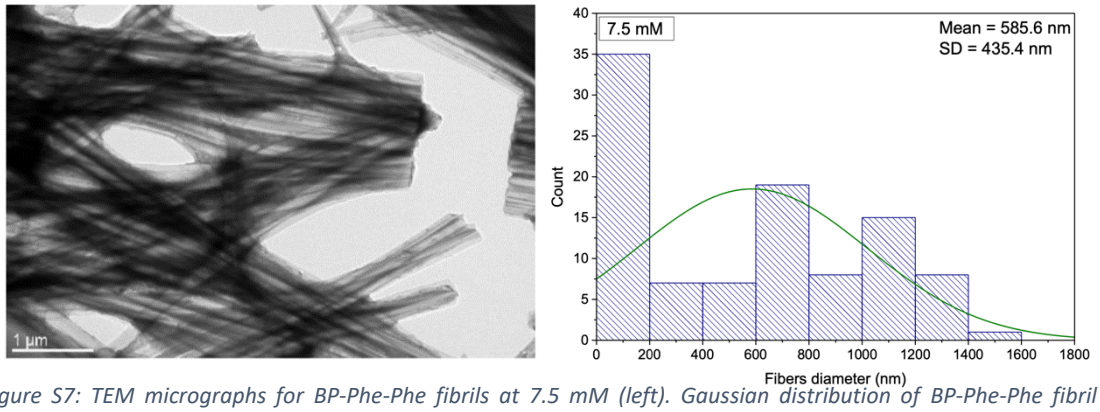

Figure S7: TEM micrographs for BP-Phe-Phe fibrils at 7.5 mM (left). Gaussian distribution of BP-Phe-Phe fibril diameter at the concentration of 7.5 mM (right).

- Fibers at 10 mM

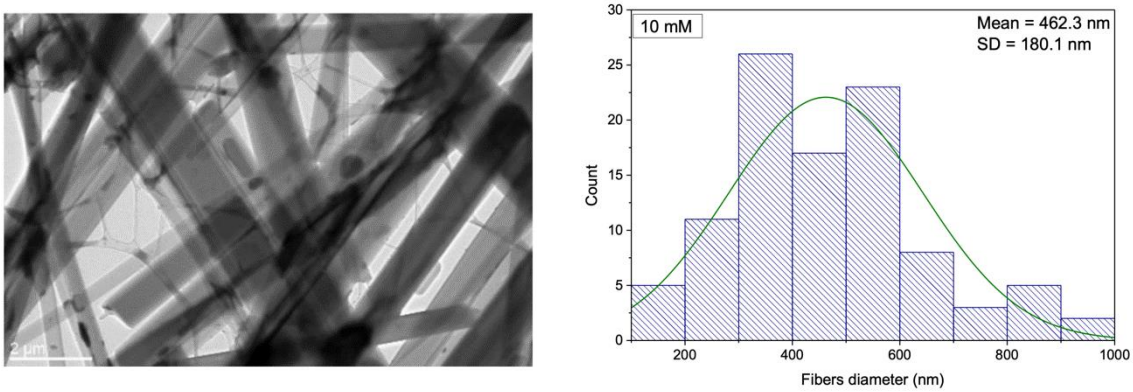

Figure S8: TEM micrographs for BP-Phe-Phe fibrils at 10 mM (left). Gaussian distribution of BP-Phe-Phe fibril diameter at the concentration of 10 mM (right).

6. X-Ray Diffraction (XRD) single crystal structure

Description

The asymmetric unit contains a single molecule of the compound, with the carboxyl moiety of the second phenylalanine residue in its protonated form. No further electron density is present in the asymmetric unit. A total of 4 molecules of peptide, related by symmetry operators of the $P2_12_12_1$ space group, are present in the unit cell (**Figure S9**).

The crystal packing shows a prevalent hydrophobic character of the whole structure, with smaller hydrophilic regions including the peptide backbone and C-terminus (**Figure S10**). Strong hydrophilic interactions are present between the molecules, namely hydrogen bonds involving the backbone carbonyl and amino moieties and the carboxyl terminus of the dipeptide (**Figure S9**, black dashes). These interactions hold together the molecules in perpendicular directions, as hydrogen bonds involving the backbone are oriented along the *a* crystallographic direction, while hydrogen bonds involving the terminal carboxylic group are oriented along the *bc* diagonal direction. The short donor-acceptor distances indicate strong hydrogen bonding interactions. Despite the highly hydrophobic character of the molecules, hydrophobic interactions are less evident. Piles of phenyl rings (**Figure S11**) suggest the presence of π-π stacking interactions. However, the quite long center-to-center distance (5 Å) and the significant offset between the rings (4 Å) indicate that these interactions are significantly weaker than the hydrogen bonding interactions.

a)

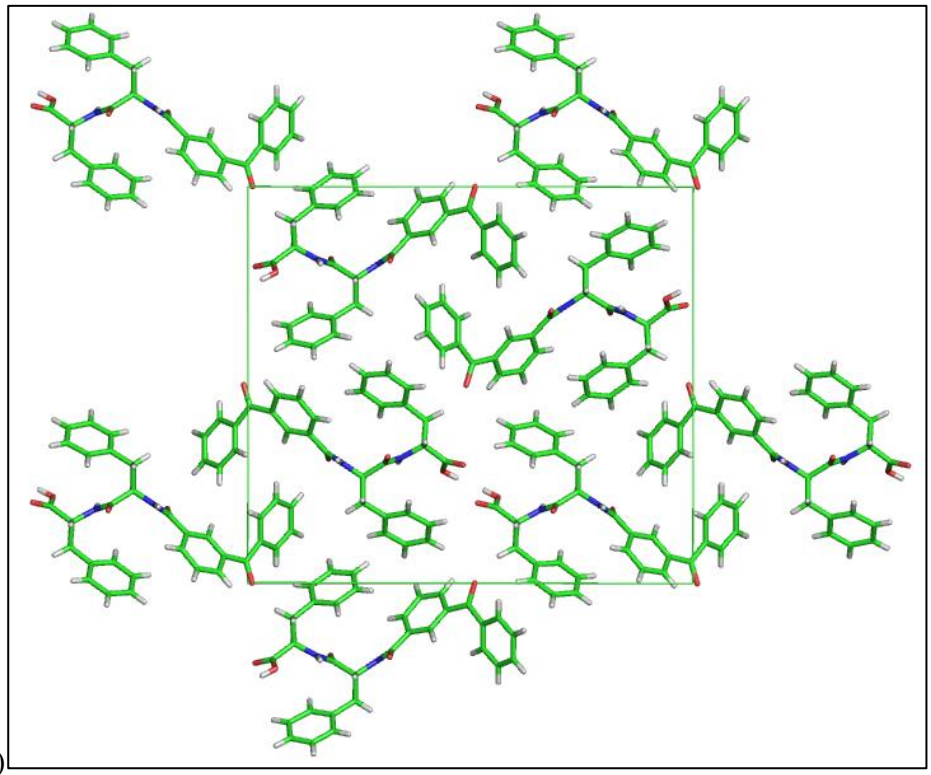

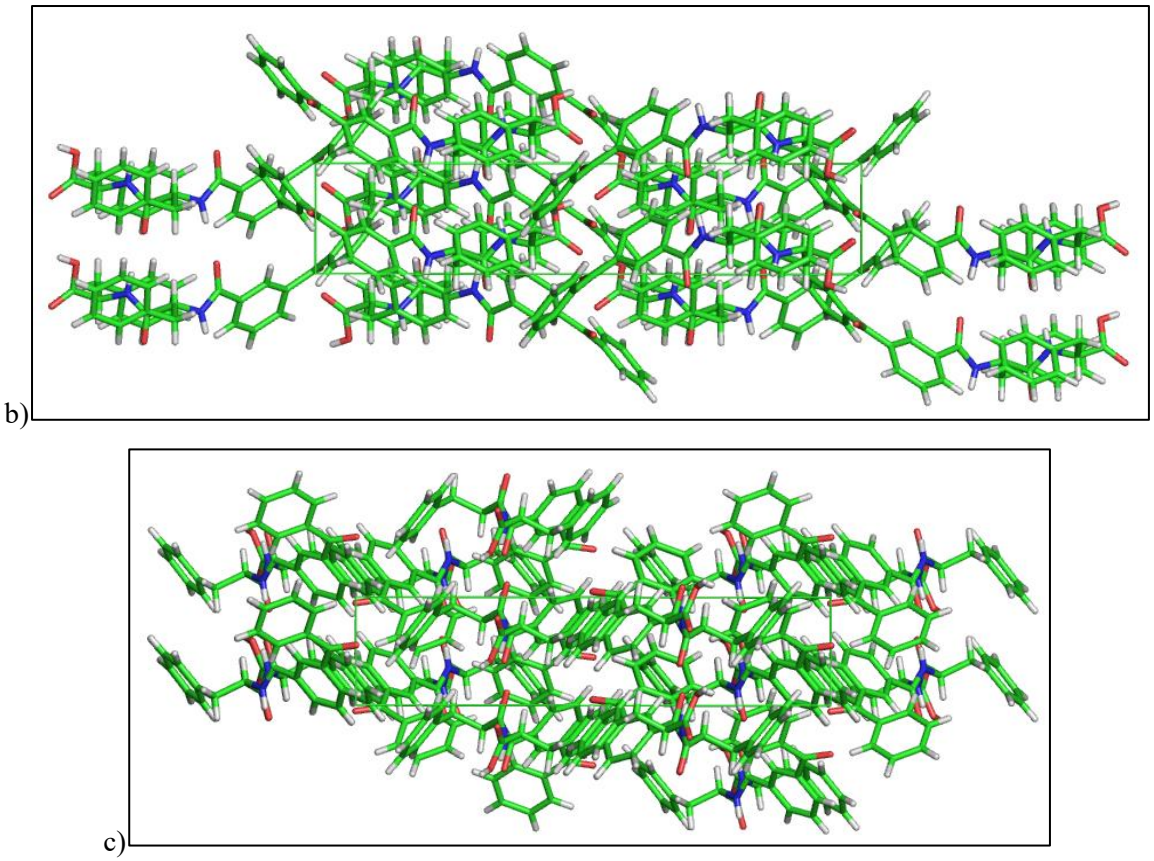

Figure S9: Unit cell of crystals of BP-Phe-Phe. Crystal packing in the crystal of the compound BP-Phe-Phe, grown in acetonitrile and water. Views along a crystallographic axis (a), the b crystallographic axis (b) and the c crystallographic axis (c). Carbon atoms are shown in green, oxygen atoms in red, nitrogen atoms in blue, hydrogen atoms in white.

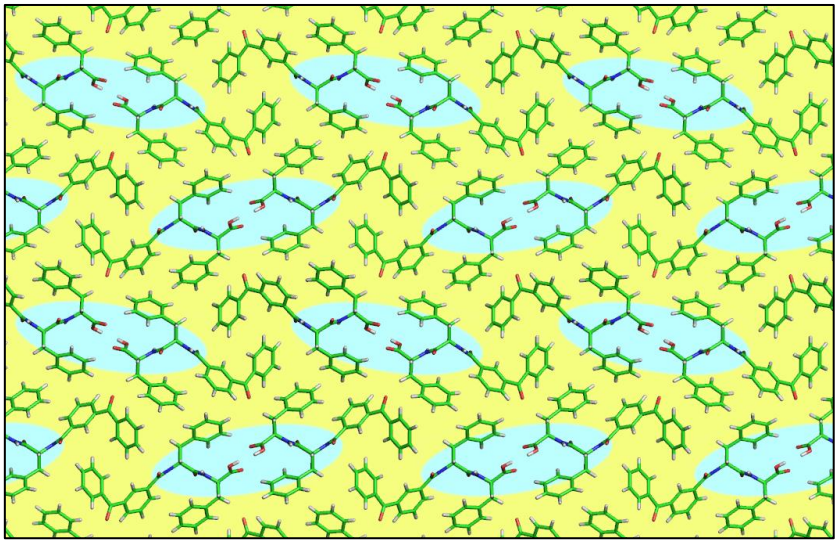

Figure S10: Crystal packing in the structure of BP-Phe-Phe. Hydrophilic and hydrophobic regions are shown with light blue and yellow background, respectively. Crystal packing is shown along a crystallographic direction.

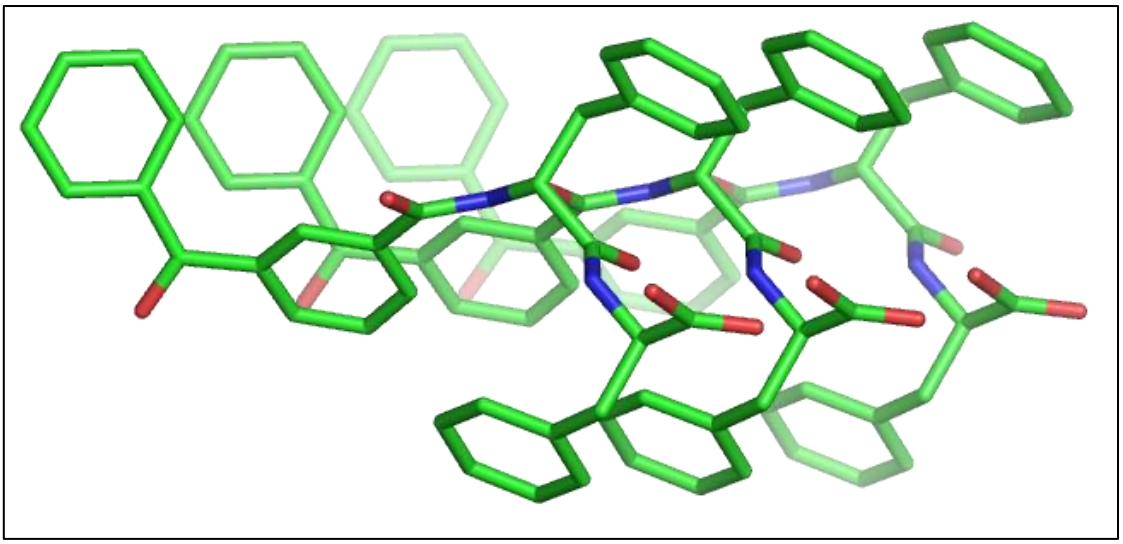

Figure S11: Hydrophobic interactions. π stacking interactions are present in the crystal structure and involve the phenyl rings of the benzophenone as well as of the phenylalanine residues. In each case, a pile of phenyl rings is formed, with a center-to-center distance of 4.9 Å, an offset of about 4 Å and an angle between the plane of each phenyl ring and the center-to-center segment of about 60°.

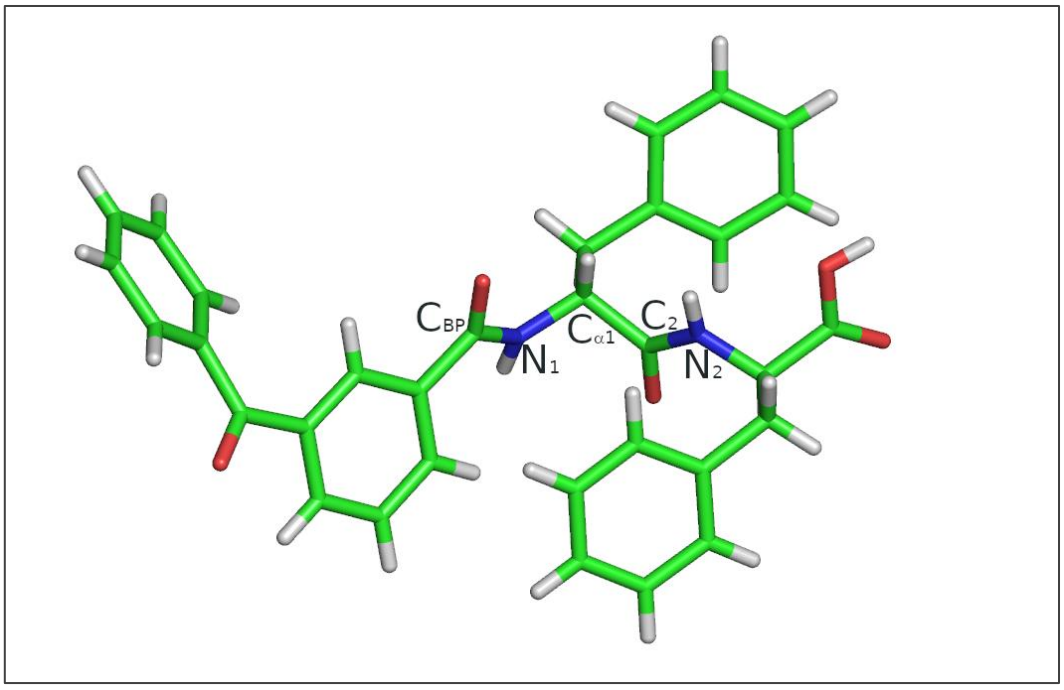

*Figure S12: Representation of the crystallographic structure of the compound BP-Phe-Phe **1** highlighting atoms involved in the torsion angles comparable to the φ and ψ torsion angles of proteins, C_{BP}-N_1-$C_{\alpha 1}$-C_1 and N_1-$C_{\alpha 1}$-C_1-N_2, respectively.*

Crystallographic details

A needle-shaped single crystal of the peptide was collected with a loop, cryoprotected by dipping the crystal in glycerol and stored frozen in liquid nitrogen. The crystal was mounted on the diffractometer at the synchrotron Elettra, Trieste (Italy), beamline XRD1, using the robot present at the facility. Temperature was kept at 100 K by a stream of nitrogen on the crystal. Diffraction data were collected by the rotating crystal

method using synchrotron radiation, wavelength 0.70 Å, rotation interval 1°/image, crystal-to-detector distance of 85 mm. A total of 133 images were collected. Reflections were indexed and integrated using the XDS package,[3] space group $P2_12_12_1$ was determined using POINTLESS[4] and the resulting data set was scaled using AIMLESS.[5] Phase information were obtained by direct methods using the software SHELXT.[6] Refinements cycles were conducted with SHELXL-14,[7] operating through the WinGX GUI,[8] by full-matrix least-squares methods on F^2. Unit cell parameters and scaling statistics are reported in **Table S2**. The asymmetric unit contains a single molecule of the compound. Hydrogen atoms were added at geometrically calculated positions and refined isotropically, with thermal parameters dependent on those of the attached atom. The protonation state of the C-terminus of the second phenylalanine residue (protonated) was identified considering the total net charge of the unit cell and the geometry of interactions surrounding the electron density of the carboxyl moiety. During refinement, no restraints were applied on distances, angles or thermal parameters of the compound. All the atoms, except the hydrogen atoms, within the asymmetric unit have been refined with anisotropic thermal parameters. Refinement statistics are reported in **Table S2**.

	BP-Phe-Phe
Formula	$C_{32}H_{28}N_2O_5$
Temperature (K)	100
Wavelength (Å)	0.7
Crystal system	Orthorhombic
Space group	$P\ 2_1\ 2_1\ 2_1$
a (Å)	4.925(1)
b (Å)	21.683(4)
c (Å)	24.350(5)
α (°)	90
β (°)	90
γ (°)	90
V (Å^3)	2600.3(9)
Z, ρcalc (g/cm^3)	4, 1.330
μ (mm^{-1})	0.086
F (000)	1096
Data collection θ range	1.85 - 25.91
Refl. Collected / unique	11998 / 4974

Rint	0.133
Completeness (%)	96.7
Data/Restraints/Parameters	4974 / 0 / 353
GooF	0.963
R1, wR2 [I>2σ(I)]	0.0749 / 0.1767
R1, wR2 all data	**0.1538.2266**

Table S2. Crystallographic data for BP-Phe-Phe.

7. Thioflavin T assay

The fluorescence emission was measured using a TECAN Infinite M1000 pro multimode plate reader instrument, selecting an excitation wavelength of 446 nm and an emission wavelength of 490 nm, with a bandwidth of 20 nm and a gain of 100. All the samples were prepared directly inside of Nunclon 96 U Bottom Black Polystyrene plate at 25 ± 0.2 °C, using a solution of Thioflavin-T (22.2 μM in 20 mM glycine-NaOH pH 7.5, filtered with a 0.2 μm filter). Experiments were performed in triplicate wells for each concentration and repeated at least twice.

8. ATR-IR Spectroscopy

Sample was prepared at concentration 1 mM in HFPI:CH_3CN 10:90 and left to dry under vacuum overnight using a 1 cm^2 piece of silicon wafer for ATR or on a glass slide for Raman. ATR-IR spectra were acquired using an IRAffinity-1S spectrophotometer (Shimadzu) at 4 cm^{-1} resolution and 240 scans.

9. Circular dichroism (CD) spectroscopy

The formation of fibers was followed using 0.1 mm quartz cell on a *Jasco J815* spectropolarimeter, with 1 s integration and a step size of 1 nm with a bandwidth of 1 nm over a range of wavelengths from 300 to 220.

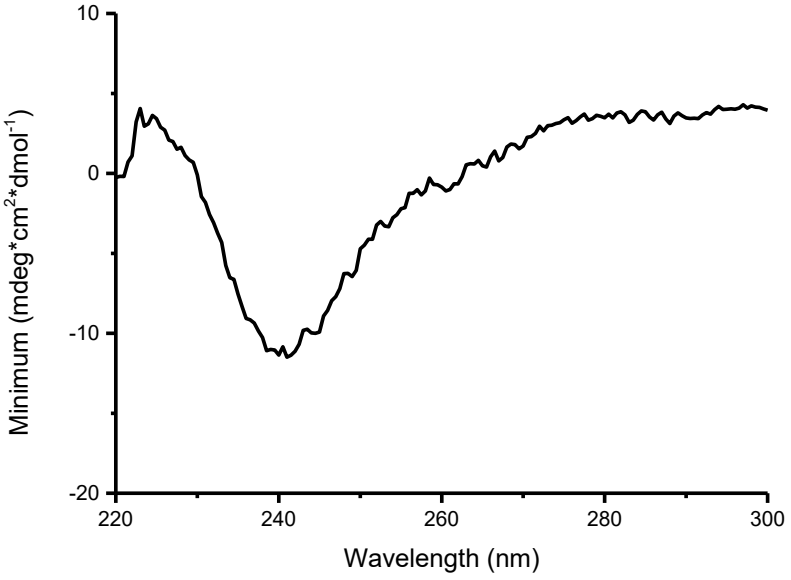

Figure S13: CD spectrum of BP-Phe-Phe.

The formation of fibers was followed by CD using 0.1 mm, 2 s integration, 4 accumulations and a step size of 1 nm with a bandwidth of 2 nm over a range of wavelengths from 300 to 220. The spectra were registered every 8 minutes for 64 minutes (Figure S13).

10. MicroRaman Spectroscopy

Dried samples were analysed by Raman spectroscopy with an *Invia Renishaw microspectrometer* (50) equipped with a 532 nm He-Ne. Laser was focus on the samples using the 50x microscope, and the power was set at 0.08 mW. Analysed range was 400-4000 cm^{-1}. At least 20 accumulations were carried out on ten different areas of the samples with an acquisition exposure time of 10 second for each accumulation.

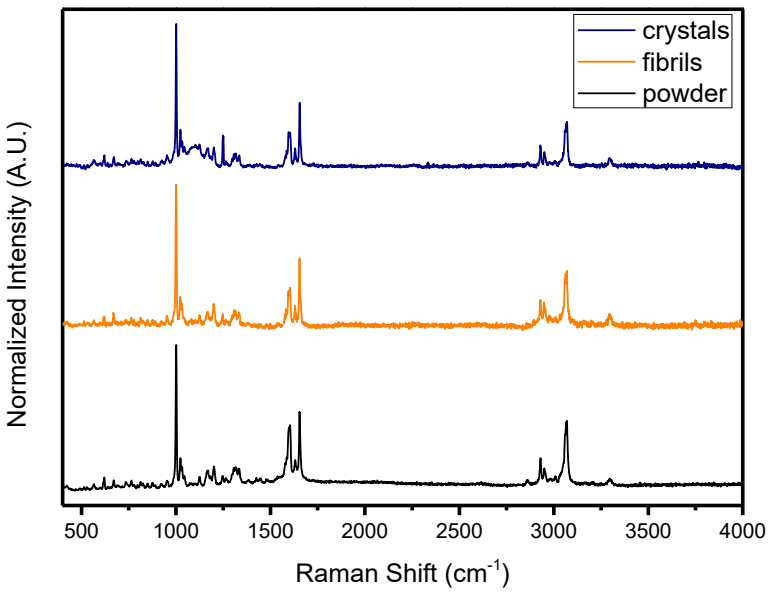

Figure S14: Raman spectra of BP-Phe-Phe

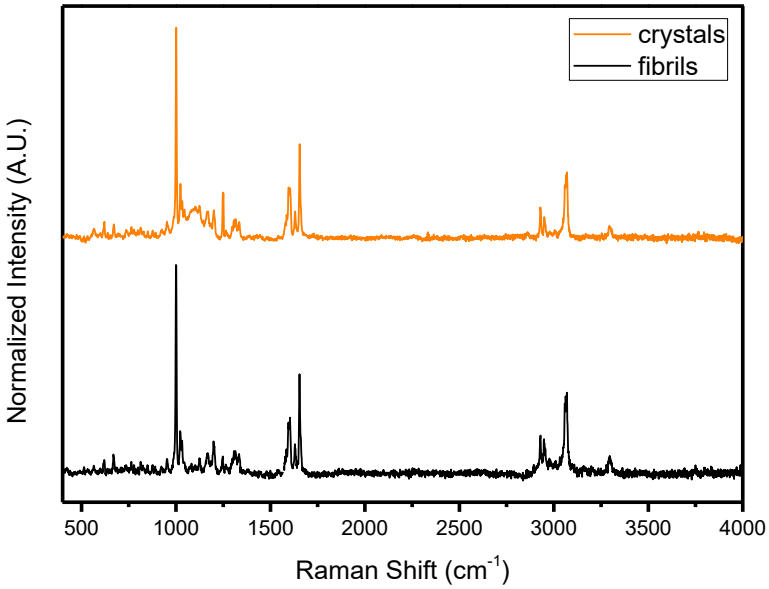

Figure S15: Visible-light Raman spectra of the BP-Phe-Phe fibrils and crystal.

11. UV-Vis and emission spectroscopy

Photophysical characterisation of BP-Phe-Phe 1

The BP-Phe-Phe **1** peptide was characterised photochemically through UV-Vis absorption and emission spectroscopy.

The absorption spectrum shows a maximum at $\boldsymbol{\lambda}_{MAX}$ = 340 nm in DMSO:MeCN, 1:1.

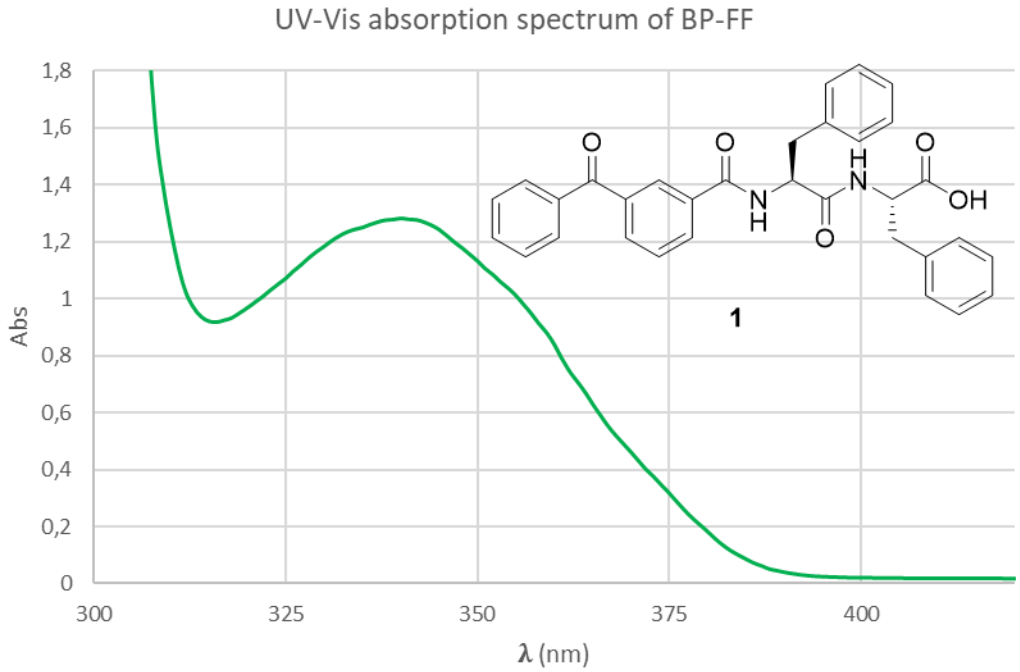

*Figure S16: UV-Vis absorption spectrum of a 10 mM solution of BP-Phe-Phe (**1**) at λMAX = 340 nm. The spectrum was registered at room temperature in DMSO:MeCN 1:1.*

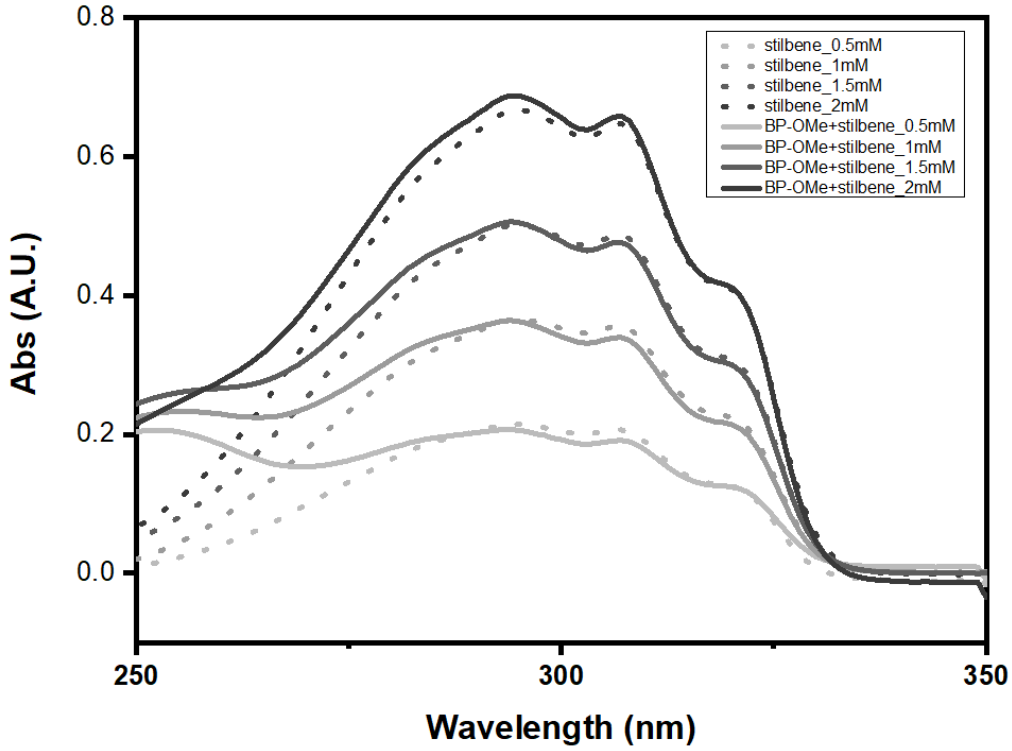

Figure S17: UV-Vis absorption spectra of stilbene without and with BP-Phe-Phe (1 mM, cac).

The emission spectrum shows a maximum at λ_{EM} = 390 nm (λ_{EXC} = 315 nm) in DMSO:MeCN, 1:1.

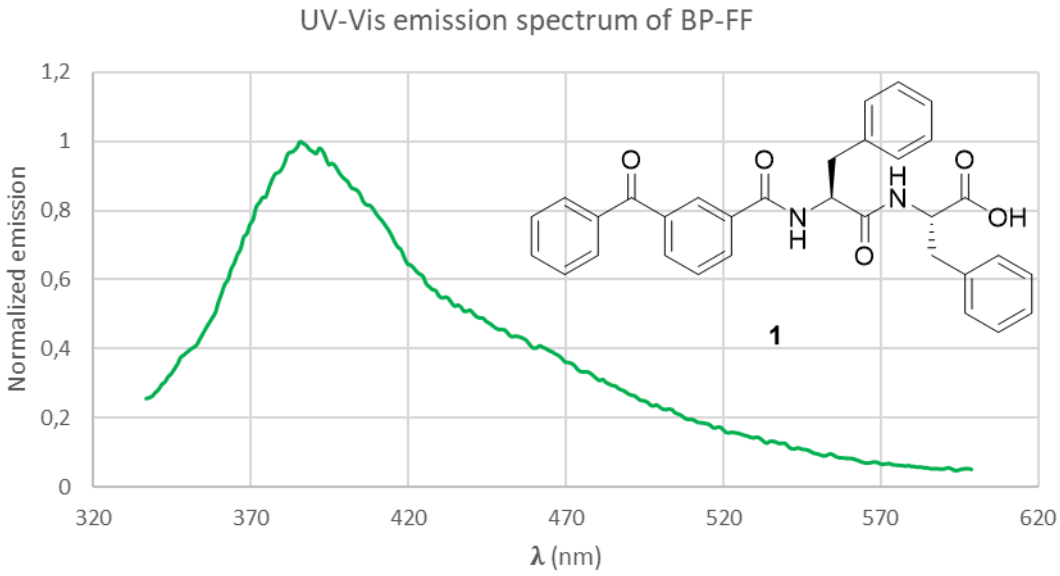

*Figure S18: Normalized emission spectrum of a 10 mM solution of BP-Phe-Phe (**1**). The spectrum was registered at room temperature in DMSO:MeCN 1:1.*

Triplet decay was measured in MeCN by laser flash photolysis (exc. at 355 nm) following the featuring transient absorption signal of the triplet excited state of BP at 530 nm: τ = 55 (±2) μs.[9]

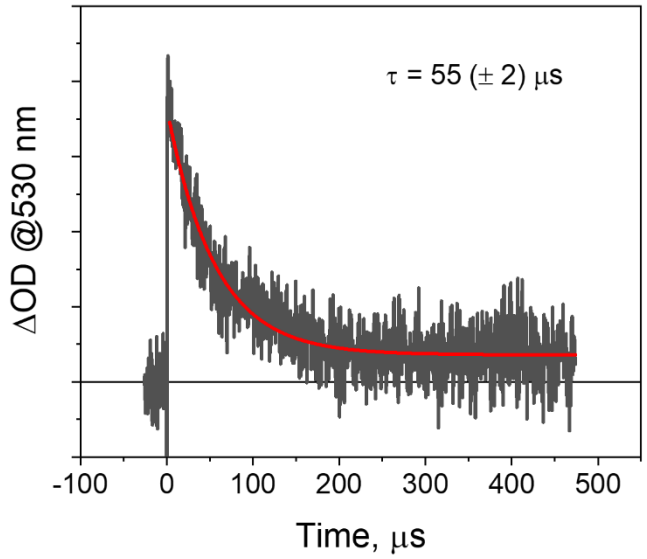

*Figure S19: Triplet decay spectrum of BP-Phe-Phe (**1**).*

Emission spectrum measured at 77 K (ethanol:methanol, 4:1):

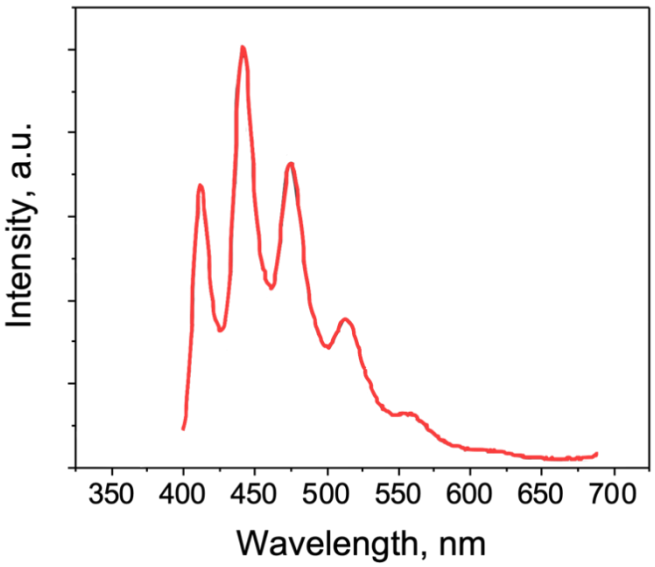

*Figure S20: Triplet state emission spectrum at 77K of BP-Phe-Phe (**1**)*

Photophysical characterisation of BP methyl ester 4

The BP methyl ester **4** was characterised photochemically through emission spectroscopy.

Emission spectrum of (**4**) with λ_{EXC} = 314 nm in DMSO:MeCN, 1:1:

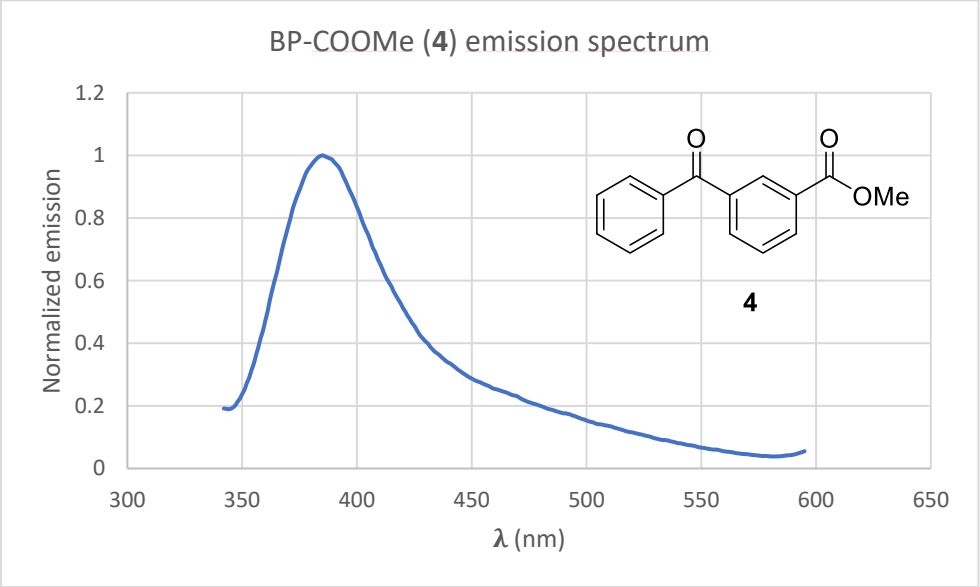

*Figure S21: UV-Vis emission spectrum of BP methyl ester (**4**) in DMSO:MeCN 1:1. λ_{EXC} = 314 nm.*

Triplet decay was measured in MeCN by laser flash photolysis (exc. at 355 nm) following the featuring transient absorption signal of the triplet excited state at 530 nm: τ = 44 (±2) *μs*.

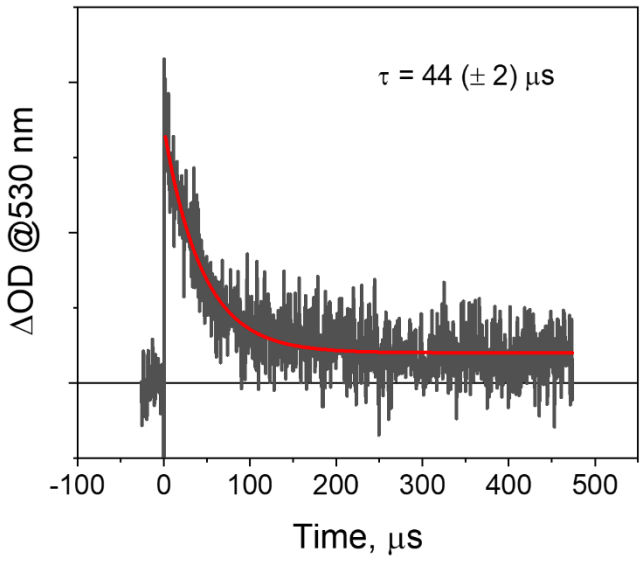

*FigureS22: Triplet decay spectrum of BP methyl ester (**4**).*

Emission spectrum measured at 77 K (ethanol:methanol, 4:1):

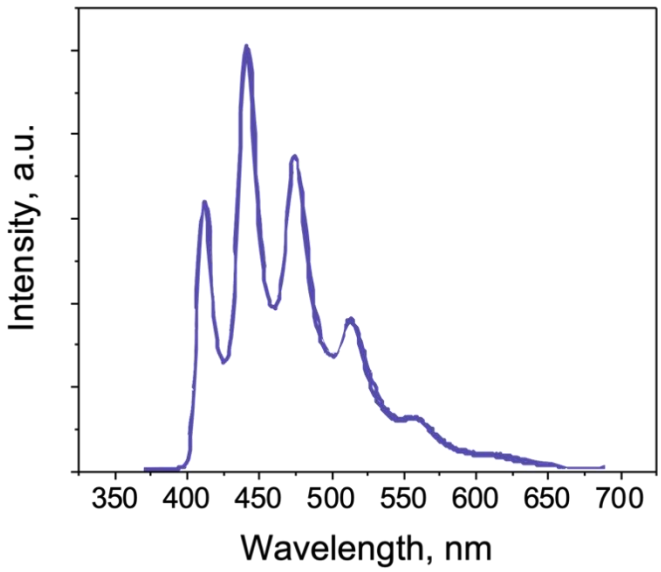

*Figure S23: Triplet state emission spectrum at 77K of BP methyl ester (**4**)*

12. UV Resonance Raman spectroscopy (UVRR)

UV Raman spectra of BP-Phe-Phe **1** and *E*-stilbene **2** in solution were collected using the UVRR setup available at the BL10.2-IUVS beamline of Elettra Sincrotrone Trieste with 266 nm as excitation wavelength. The vertically polarized VV Raman spectra were recorded in a back-scattered geometry and analysed by using a single pass of a Czerny-Turner spectrometer (Trivista 557, Princeton Instruments, 750 mm of focal length) equipped with holographic grating at 1800 g/mm and 3600 g/mm and a UV-optimised CCD camera. The calibration of the spectrometer was standardised using cyclohexane (spectroscopic grade, Sigma Aldrich). The resolution was set at 1.1 cm^{-1}/pixel. The final radiation power on the samples was kept at about 0.2 mW. Possible photo-damage effect due to prolonged exposure of the sample to UV radiation was minimised by continuously spinning the sample cell during the measurements.

13. Photoisomerisation of olefins

Reaction setup

Figure S23 shows the general setup of the reactions performed under 390nm light irradiation. A Kessil LED lamp at 50% of its maximum power was used, and the reaction vials (from 1 to 3 vials) were placed in front of the light source at 4 cm from the lamp. A mirror was placed behind the vials. To maintain a stable reaction temperature, a fan was placed above the irradiated vials.

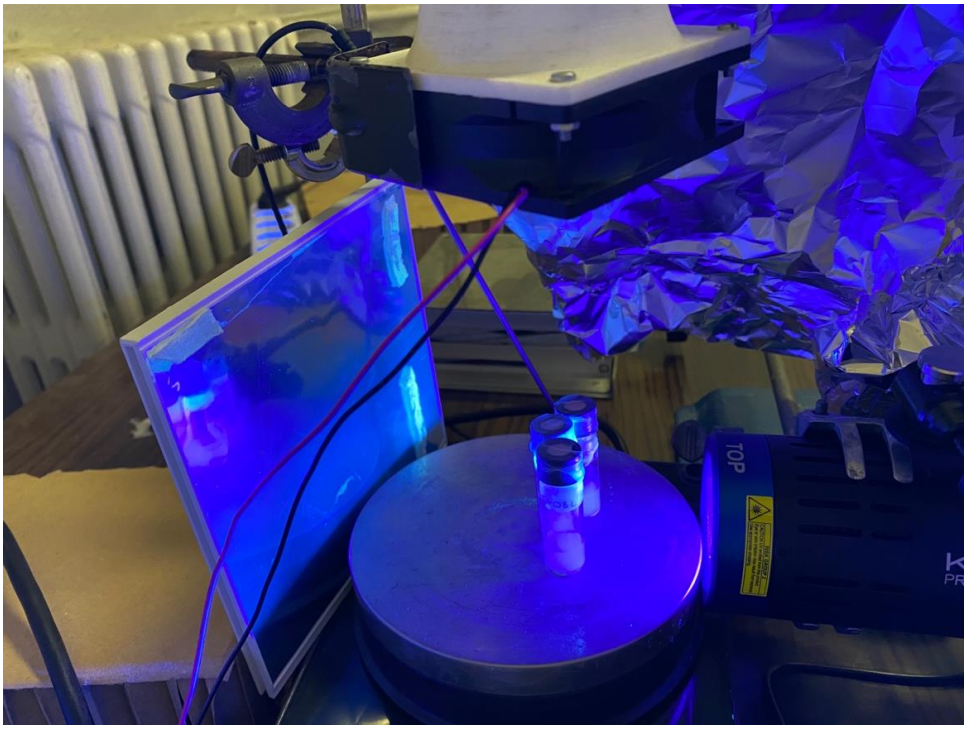

Figure S24: Reaction setup

General procedure for isomerisation of *E*-olefins:

A 4 mL screw-cap vial with a PTFE/silicone septum was charged with BP-Phe-Phe (**1**) (0.52 mg, 1 μmol, 1 mol%) and degassed under argon atmosphere for 3 minutes. Then, HFIP (100 μL) previously degassed with argon was added to dissolve the peptide. After complete dissolution at 25°C, anhydrous MeCN (900 μL) previously degassed with argon was added. After 1 hour of incubation, the desired olefin (0.1 mmol, 1 equiv.) was added. The vial was shortly degassed with argon (15 s), sealed and irradiated using a 390 nm Kessil lamp (50% intensity) placed at 4 cm distance, stirring at 50 rpm for the desired reaction time. Then, the crude product was concentrated in vacuo, dissolved in $CDCl_3$ and the yield determined by ^1H NMR spectroscopy using 1,3,5-trimethoxybenzene as internal standard.

Characterization data

(*Z*)-stilbene (*Z*-2)

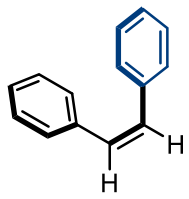

Z-**2** was synthesised according to the general procedure **A** from *E*-stilbene (*E*-**2**) (0.1 mmol) by conducting the reaction for 7 h obtaining the corresponding product in 94% NMR yield, 62:38 *Z:E* ratio. **^{1}H NMR** (400 MHz, $CDCl_3$): 7.27 – 7.21 (m, 10H), 6.63 – 6.60 (m, 2H). These data are consistent with those reported in the literature.[10]

(*Z*)-(4-styrylphenyl)methanol (*Z*-5)

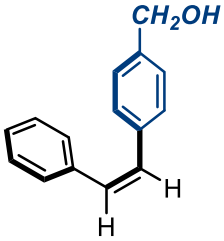

Z-**5** was synthesised according to the general procedure **A** from (*E*)-(4-styrylphenyl)methanol (*E*-**5**) (0.1 mmol) by conducting the reaction for 7 h obtaining the corresponding product in quantitative NMR yield, 50:50 *Z:E* ratio. **^{1}H-NMR** (300 MHz, $CDCl_3$): δ 7.52-7.46 (m, 2H), 7.35-7.29 (m, 2H), 7.28-7.13 (m, 5H), 6.77 (d, *J* = 12.3 Hz, 1H), 6.57 (d, *J* = 12.3 Hz, 1H), 4.62 (s, 2H). These data are consistent with those reported in the literature.[11]

(*Z*)-4-methoxystilbene (*Z*-6)

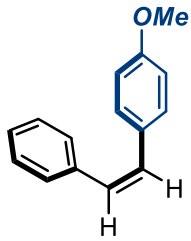

Z-**6** was synthesised according to the general procedure **A** from (*E*-)-4-methoxystilbene (*E*-**6**) (0.1 mmol) by conducting the reaction for 7 h obtaining the corresponding product in 97% NMR yield, 33:67 *Z:E* ratio. **^{1}H NMR** (500 MHz, $CDCl_3$): δ 7.28 – 7.14 (m, 7H), 6.74 (d, *J* = 8.8 Hz, 2H), 6.51 (s, 2H), 3.76 (s, 3H). These data are consistent with those reported in the literature.[10]

(*Z*)-4-bromostilbene (*Z*-7)

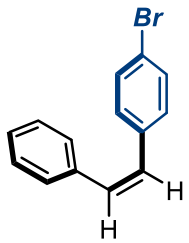

Z-**7** was synthesised according to the general procedure **A** from (*E*)-4-bromostilbene (*E*-**7**) (0.1 mmol) by conducting the reaction for 7 h obtaining the corresponding product in quantitative NMR yield, 19:81 *Z:E* ratio. **^{1}H NMR** (400 MHz, $CDCl_3$): δ 7.33 (d, *J* = 8.4 Hz, 2H), 7.26 – 7.18 (m, 5H), 7.10 (d, *J* = 8.3 Hz, 2H), 6.63 (d, *J* = 12.0 Hz, 1H), 6.49 (d, *J* = 12.1 Hz, 1H). These data are consistent with those reported in the literature.[12]

methyl (*Z*)-3-phenylacrylate (*Z*-8)

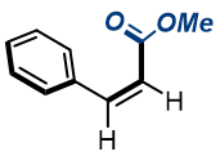

Z-**8** was synthesised according to the general procedure **A** from (methyl (*E*)-3-phenylacrylate (*E*-**8**) (0.1 mmol) by conducting the reaction for 24 h obtaining the corresponding product in 95% NMR yield, 58:42 *Z:E* ratio. **^{1}H NMR** (400 MHz, $CDCl_3$): δ 7.60 (dd, *J* = 7.5, 1.7 Hz, 2H), 7.38 – 7.33 (m, 3H), 6.97 (d, *J* = 12.6 Hz, 1H), 5.97 (d, *J* = 12.6 Hz, 1H), 3.72 (s, 3H). These data are consistent with those reported in the literature.[13]

(*Z*)-ethyl cinnamate (*Z*-9)

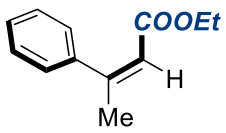

Z-**9** was synthesised according to the general procedure **A** from (*E*)-ethyl cinnamate (*E*-**9**) (0.1 mmol) by conducting the reaction for 24 h obtaining the corresponding product in 96% NMR yield, 75:25 *Z:E* ratio. **^{1}H NMR** (400 MHz, $CDCl_3$): δ 7.37 - 7.29 (m, 3H), 7.22 - 7.20 (m, 2H), 5.91 (s, 1H), 4.00 (q, *J* = 7.2 Hz, 2H), 2.18 (s, 3H), 1.08 (t, *J* = 7.2 Hz, 3H). These data are consistent with those reported in the literature.[14]

(*Z*)-cinnamonitrile (*Z*-10)

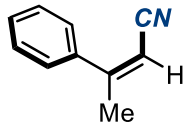

Z-**10** was synthesised according to the general procedure **A** from (*E*)-cinnamonitrile (*E*-**10**) (0.1 mmol) by conducting the reaction for 24 h obtaining the corresponding product in 93% NMR yield, 61:39 *Z:E* ratio. **^{1}H NMR** (400 MHz, $CDCl_3$): 7.82 - 7.79 (m, 2H), 7.50 – 7.40 (m, 3H), 5.44 (q, *J* = 1.6 Hz, 1H), 2.32 (d, *J* = 1.4 Hz, 3H). These data are consistent with those reported in the literature.[15]

(*Z*)-1-phenyl-2-(trimethylsilyl)ethylene (*Z*-11)

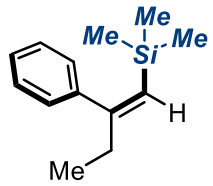

Z-**11** was synthesised according to the general procedure **A** from (*E*)-1-phenyl-2-(trimethylsilyl)ethylene (*E*-**11**) (0.1 mmol) by conducting the reaction for 7 h obtaining the corresponding product in 72% NMR yield, 72:28 *Z:E* ratio. **^{1}H NMR** (400 MHz, $CDCl_3$): 7.43-7.21 (m, 3H), 7.21 – 7.03 (m, 2H), 5.57 (t, *J* = 1.4 Hz, 1H), 2.43 (qd, *J* = 7.4, 1.4 Hz, 2H), 1.04 (t, *J* = 7.4 Hz, 3H), -0.17 (s, 9H). These data are consistent with those reported in the literature.[16]

14. Unsuccesful substrates

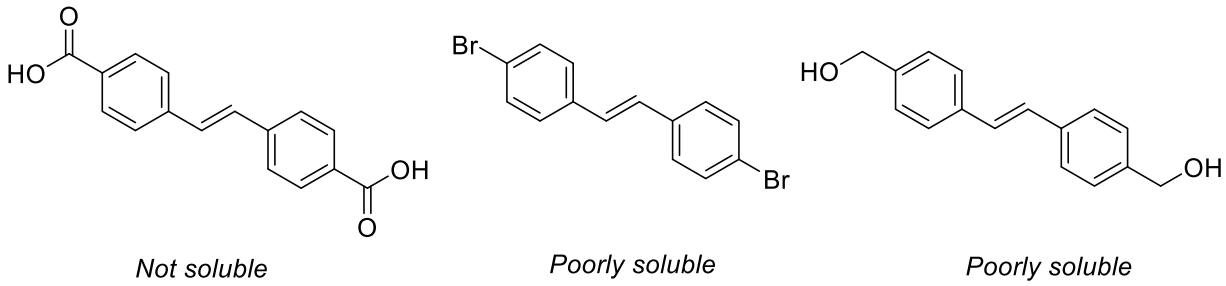

Not soluble *Poorly soluble* *Poorly soluble*

Figure S25: Unsuccessful substrates.

15. References

1 I. Degani, S. Dughera, R. Fochi and S. Gazzetto, *J. Org. Chem.*, 1997, **62**, 7228–7233.

2 O. Exner, H. Dahn and P. Péchy, *Magn. Reson. Chem.*, 1992, **30**, 381–386.

3 W. Kabsch, *Acta Crystallogr., Sect. D.*, 2010, **66**, 125–132.

4 P. Evans, *Acta Crystallogr. Sect. D Biol. Crystallogr.*, 2006, **62**, 72–82.

5 P. R. Evans and G. N. Murshudov, *Acta Crystallogr. Sect. D Biol. Crystallogr.*, 2013, **69**, 1204–1214.

6 G. M. Sheldrick, *Acta Crystallogr. Sect. A Found. Crystallogr.*, 2008, **64**, 112–122.

7 G. M. Sheldrick, *Acta Crystallogr. Sect. C Struct. Chem.*, 2015, **71**, 3–8.

8 L. J. Farrugia, *J. Appl. Crystallogr.*, 2012, **45**, 849–854.

9 I. Carmichael and G. L. Hug, *J. Phys. Chem. Ref. Data*, 1986, **15**, 1–250.

10 S. Bognar and M. van Gemmeren, *Chem. - A Eur. J.*, , DOI:10.1002/chem.202203512.

11 B. Xiao, Z. Niu, Y. G. Wang, W. Jia, J. Shang, L. Zhang, D. Wang, Y. Fu, J. Zeng, W. He, K. Wu, J. Li, J. Yang, L. Liu and Y. Li, *J. Am. Chem. Soc.*, 2015, **137**, 3791–3794.

12 M. Das and D. F. OShea, *Org. Lett.*, 2016, **18**, 336–339.

13 J. J. Zhong, Q. Liu, C. J. Wu, Q. Y. Meng, X. W. Gao, Z. J. Li, B. Chen, C. H. Tung and L. Z. Wu, *Chem. Commun.*, 2016, **52**, 1800–1803.

14 Y. M. Wei, X. Di Ma, L. Wang and X. F. Duan, *Chem. Commun.*, 2020, **56**, 1101–1104.

15 X. Huang and N. Jiao, *Org. Biomol. Chem.*, 2014, **12**, 4324–4328.

16 T. M. T. Le, T. Brégent, P. Jubault and T. Poisson, *Chem. - A Eur. J.*, 2022, **28**, e202201514.